Available online at www.sciencedirect.com
ScienceDirect
Journal of Power Sources 180 (2008) 199–204
JOURNAL OF POWER SOURCES
www.elsevier.com/locate/jpowsour

Short communication

The effect of carbon support treatment on the stability of Pt/C electrocatalysts

Weimin Chen [a,*], Qin Xin [b], Gongquan Sun [c], Qi Wang [c], Qing Mao [c], Huidong Su [a]

[a] School of Environmental and Chemical Engineering, Shenyang Ligong University, Shenyang 110168, China
[b] State Key Laboratory of Catalysis, Dalian Institute of Chemical Physics, Chinese Academy of Sciences, Dalian 116023, China
[c] Direct Alcohol Fuel Cell Laboratory, Dalian Institute of Chemical Physics, Chinese Academy of Sciences, Dalian 116023, China

Received 11 December 2007; received in revised form 2 February 2008; accepted 4 February 2008
Available online 13 February 2008

Abstract

A potential cycling test was conducted to evaluate the effect of carbon support treatment on the stability of Pt/C electrocatalysts. The FTIR spectra show that after oxidative treatments, the carbon support became rich in oxygen-containing functional groups. Oxidative treatments of the carbon support increase the interaction between the metal particle and the support, resulting in an improved electrochemical stability of Pt/C catalysts. The Pt/C catalyst prepared from the H_2O_2-treated carbon support exhibits a higher stability than that prepared from the HNO_3-treated carbon support.

Keywords: Electrocatalyst; Stability; Carbon support; Surface treatment; Potential cycling test

1. Introduction

Low-temperature fuel cells including polymer electrolyte fuel cells (PEFCs) and direct alcohol fuel cells (DAFCs) are promising power sources due to their advantages such as high energy efficiency, good portability and ambient operating conditions [1–4]. Pt-based metal catalysts are widely used as electrocatalysts in low-temperature fuel cells. The nano-sized metal particles are unstable under the electrochemical stress. During long-term operations, metal particles agglomerate gradually, resulting in catalytic activity losses [5,6]. For supported metal catalysts, the interaction between the metal particle and the support is a dominant factor influencing the sintering process of the metal particles. Wu et al. [7] observed that the Pt–support interaction was stronger in Pt-SWNTs catalysts than in Pt-XC-72 and Pt-MWNT catalysts. Yu et al.'s results [8] show that the H_2SO_4–HNO_3 treatment produces functional groups on the surface of carbon nanotubes and these surface functional groups provide active sites for interaction with metal precursors. The oxidative treatment of the support is considered to be a useful method for increasing the interaction between the metal particle and the carbon support. In this work, the carbon support was treated with H_2O_2 and HNO_3, and the potential cycling test was conducted to evaluate the electrochemical stabilities of Pt/C catalysts.

The potential cycling test is widely used to rapidly evaluate the stability of electrocatalysts [9–11]. In this work, the potential cycling test was conducted within the potential range of 0.6–1.05 V, which is a typical potential range of the cathode in low-temperature fuel cells. Electrochemical and physical characterizations were carried out before and after the potential cycling test.

2. Experimental

2.1. Support treatment and catalyst preparation

A commercial carbon black (Vulcan XC-72, Cabot Corp.) was treated with H_2O_2 and HNO_3, respectively. For the H_2O_2 treatment, the carbon black was refluxed in 10 wt.% H_2O_2 solution at 105 °C for 3 h, and for the HNO_3 treatment, the carbon black was refluxed in 65 wt.% HNO_3 solutions at 120 °C for 3 h. Treated carbon blacks were filtered and washed with deionized water, and then they were dried at 110 °C in an oven for 12 h.

* Corresponding author. Tel.: +86 24 24692981; fax: +86 24 24692981.
E-mail address: cwm222@163.com (W. Chen).

0378-7753/$ – see front matter © 2008 Elsevier B.V. All rights reserved.
doi:10.1016/j.jpowsour.2008.02.005

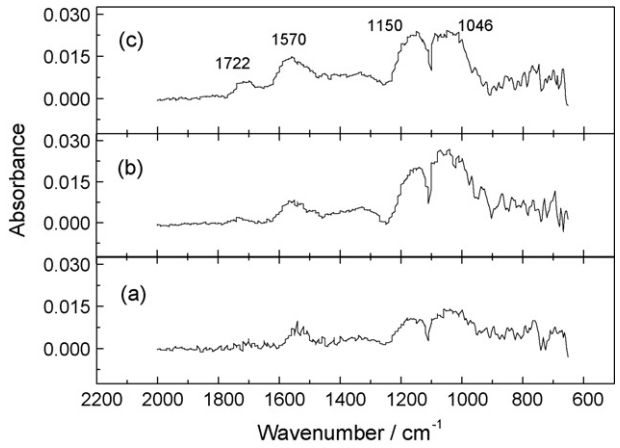

Fig. 1. FTIR spectra of carbon supports. (a) untreated Vulcan XC-72; (b) H_2O_2-treated Vulcan XC-72; (c) HNO_3-treated Vulcan XC-72.

The Pt/C catalyst was prepared using an ethylene glycol reduction method [12]. The Pt content was 40 wt.%. The Pt/C catalyst prepared from the H_2O_2-treated carbon support and that prepared from the HNO_3-treated carbon support were labeled as Pt/Vulcan-O and Pt/Vulcan-N, respectively. The Pt/C catalyst prepared from untreated support was labeled as Pt/Vulcan.

2.2. Potential cycling test

The potential cycling test was conducted in a single cell with an active cross-sectional area of 4 cm^2. A commercial polymer electrolyte membrane (Nafion® 117, DuPont Corp.) was used as the solid electrolyte. The Pt/C catalyst was mixed with 5 wt.% Nafion® ionomer solution (EW = 1100, DuPont Corp.) ultrasonically and brushed onto one side of the membrane with the Pt loading of 1 mg cm^{-2} and served as the working electrode. A commercial Pt black (HiSPEC1000, Johnson Matthey Corp.) was mixed with 5 wt.% Nafion® ionomer solution (EW = 1100, DuPont Corp.) and brushed onto the other side of the membrane and served as the counter/reference electrode. The potential cycling test was conducted within the potential range of 0.6–1.05 V, with the scan rate of 20 mV s^{-1}. The temperature was 60 °C. The CV curves were recorded by a potentiostat/galvanostat (EG&G Model 273A). The working electrode was fed with degassed deionized water with the flow rate of 1 ml min^{-1}. The counter/reference electrode was fed with 0.1 MPa humidified hydrogen gas with the flow rate of 80 ml min^{-1} and designated as a dynamic hydrogen electrode (DHE). During the potential cycling test, the CV curves were recorded periodically.

After the potential cycling test, the single cell was disassembled. The Pt black was replaced by a commercial PtRu/C catalyst (HiSPEC 7000, Johnson Matthey Corp.) with the Pt loading of 1.33 mg cm^{-2}. The electrode preparation method was the same as described above. The PtRu/C catalyst served as the anode of the direct methanol fuel cell (DMFC), and the Pt/C catalyst that had undergone the potential cycling test served as the cathode. The single cell was reassembled and the discharge test of the DMFC was conducted at the temperature of 75 °C. The anode

Table 1
ECA values and mean particle sizes of Pt/C catalysts before and after the potential cycling test

Electrocatalysts	ECA (m^2 g^{-1} Pt)		Mean particle size (nm)	
	Before test	After test	Before test	After test
Pt/Vulcan	56.8	34.9	2.5	5.9
Pt/Vulcan-O	56.0	38.4	2.6	4.6
Pt/Vulcan-N	54.1	37.4	3.0	4.8

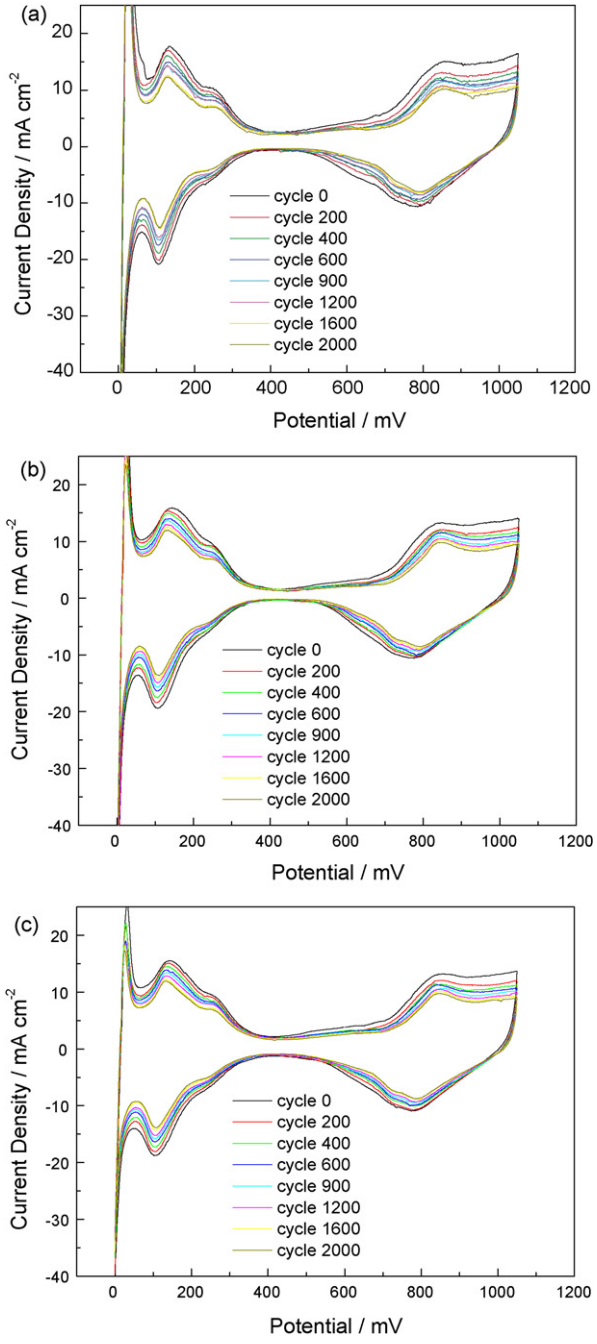

Fig. 2. CV curves of Pt/C catalysts during the potential cycling test. 60 °C, 20 mV s^{-1}: (a) Pt/Vulcan; (b) Pt/Vulcan-O; (c) Pt/Vulcan-N.

was fed with 1 mol l^{-1} methanol solution with the flow rate of 1 ml min^{-1}, and the cathode was fed with 0.2 MPa oxygen with the flow rate of 200 ml min^{-1}.

2.3. Characterization

The FTIR spectra of carbon supports were collected on a Nicolet Avatar-370 equipped with a DTGS detector and a ZnSe crystal (45° angle) as attenuated total reflection (ATR) accessory. ATR mode was adopted to obtain the spectra of carbon supports. All spectra were collected with Omnic 6.1a software. Transmission electron microscopy (TEM) investigations were carried out using a JEOL JEM-2000EX microscope operating at 120 kV. X-ray diffraction (XRD) measurements were performed on a Rigaku X-3000 X-ray diffractometer using Cu Kα radiation with a Ni filter. The tube voltage was maintained at 40 kV, and tube current at 100 mA. The 2θ angular region between 20° and 85° was explored at a scan rate of 5° min^{-1}, with the resolution of 0.02°. The Pt (2 2 0) peak (63–73°) was scanned at 1° min^{-1} to obtain the catalyst particle sizes.

3. Results and discussion

The FTIR spectra of carbon supports obtained before and after oxidative treatments are shown in Fig. 1. The bands at 1150 and 1046 cm^{-1} corresponding to the C–O stretching vibration increased after oxidative treatments of the carbon support, as shown in (b) and (c), especially in (b). On the other hand, the 1722 cm^{-1} band corresponding to the stretching vibration of carboxyl groups and the 1570 cm^{-1} band corresponding to the ionoradical structures of C=O increased considerably after the HNO_3 treatment, as shown in (c). It seems that the H_2O_2 treatment makes the support surface rich in weak acid groups, while the HNO_3 treatment makes the support surface rich in both weak acid groups and strong acid groups. This result is in accordance with the results reported by other groups [13,14].

During the potential cycling test, CV curves were recorded periodically, as shown in Fig. 2. With the increase of the scan cycle number, the hydrogen adsorption/desorption peak area declines monotonously. Pt/Vulcan-O (b) and Pt/Vulcan-N (c) exhibit higher stabilities than Pt/Vulcan (a). The electrochemical area (ECA) value of Pt/C catalysts was calculated from

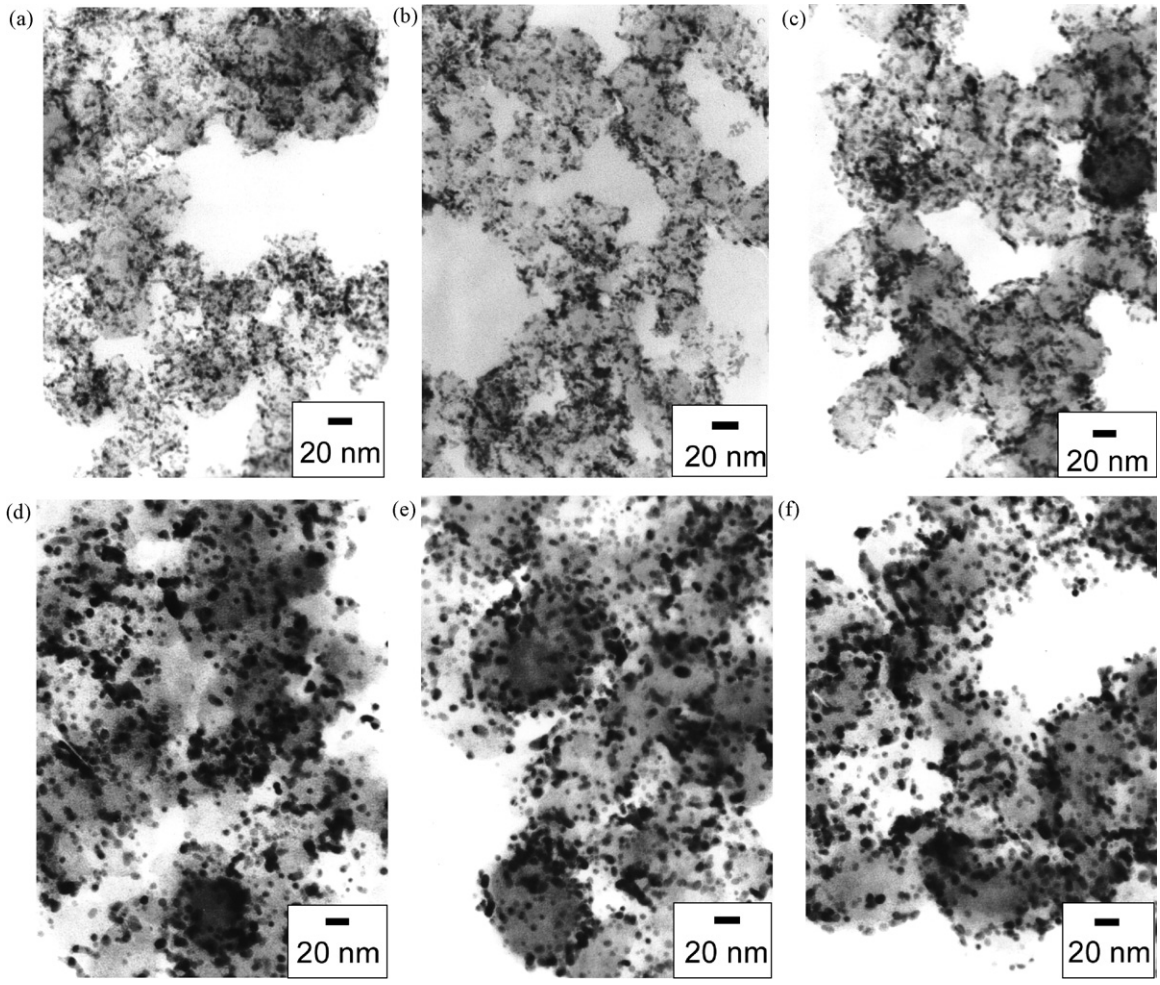

Fig. 3. TEM images of Pt/C catalysts. (a) Pt/Vulcan before potential cycling; (b) Pt/Vulcan-O before potential cycling; (c) Pt/Vulcan-N before potential cycling; (d) Pt/Vulcan after potential cycling; (e) Pt/Vulcan-O after potential cycling; (f) Pt/Vulcan-N after potential cycling.

the integrated area of the hydrogen-desorption peak, supposing an average value (210 μC cm^{-2}) for the charge associated with monolayer formation of hydrogen atoms on a polycrystalline platinum surface. The ECA values obtained before and after the potential cycling test are listed in Table 1. It is clearly seen that the ECA losses of Pt/Vulcan-O and Pt/Vulcan-N are much lower than that of Pt/Vulcan. Obviously, the electrochemical stabilities of Pt/Vulcan-O and Pt/Vulcan-N are higher than that of Pt/Vulcan, and Pt/Vulcan-O has the highest electrochemical stability.

TEM images of Pt/C catalysts before and after the potential cycling test are shown in Fig. 3. It is noteworthy that the particle size of the as-prepared Pt/Vulcan-N (c) is larger than that of the as-prepared Pt/Vulcan (a) and Pt/Vulcan-O (b). This difference may be ascribed to the low-surface area value of the HNO_3-treated carbon support. Aksoylu et al.'s result [15] shows that the HNO_3 oxidation leads to a decrease in the micropore volume of the carbon support. Gómez de la Fuente et al. [16] found that the HNO_3 treatment yields to a significant reduction of the BET area. After the potential cycling test, the Pt particle size increased remarkably, implying a severe agglomeration of Pt particles under the electrochemical stress. The Pt particles are smaller in Pt/Vulcan-O (e) and Pt/Vulcan-N (f) than in Pt/Vulcan (d).

X-ray diffraction patterns of Pt/C catalysts before and after the potential cycling test are shown in Fig. 4. Diffraction peaks located at 2θ value of 39.8, 46.1, 67.5 and 81.4° are ascribed to the facecentered cubic (fcc) facets of Pt(1 1 1), Pt(2 0 0), Pt(2 2 0) and Pt(3 1 1), respectively. The Pt(2 2 0) peak was selected to calculate the mean particle sizes of catalyst particles because it is isolated from the diffraction peaks of the carbon support and the Nafion® polymer electrolyte. The mean particle size was calculated according to Scherrer's formula [17]:

$$d = \frac{0.9\lambda_{k\alpha 1}}{B_{2\theta}\cos\theta_{\max}} \quad (1)$$

where $\lambda_{k\alpha 1}$ is the wavelength of X-ray (1.5418 Å), $\theta_{\max}$ the angle at the peak maximum, and $B_{2\theta}$ is the width (rad) of the peak at half height.

From the insets of Fig. 4, it is clearly seen that after the potential cycling test, the width of the Pt(2 2 0) diffraction peak decreased noticeably, indicating a drastic agglomeration of Pt particles. Table 1 listed particle size values of Pt/C catalysts before and after the potential cycling test. Evidently, the sintering rates of Pt/Vulcan-O and Pt/Vulcan-N were lower than that of Pt/Vulcan during the test. This result implies that the electrochemical stability of Pt/C catalysts is closely related to the interaction between the metal particle and the support surface, and high electrochemical stabilities might be achieved by the surface treatment of the support. It is noticeable that the stability of Pt/Vulcan-O is higher than that of Pt/Vulcan-N. This difference may be attributed to different functional groups on the H_2O_2-treated and HNO_3-treated carbon supports. Aksoylu et al.'s results [18] show that compared with strong acid groups, weak acid groups increase the interaction between the metal particle and the support surface more efficiently. So the higher stability of Pt/Vulcan-O than Pt/Vulcan-N might be ascribed to the high density of weak acid groups on the surface of the H_2O_2-treated carbon support.

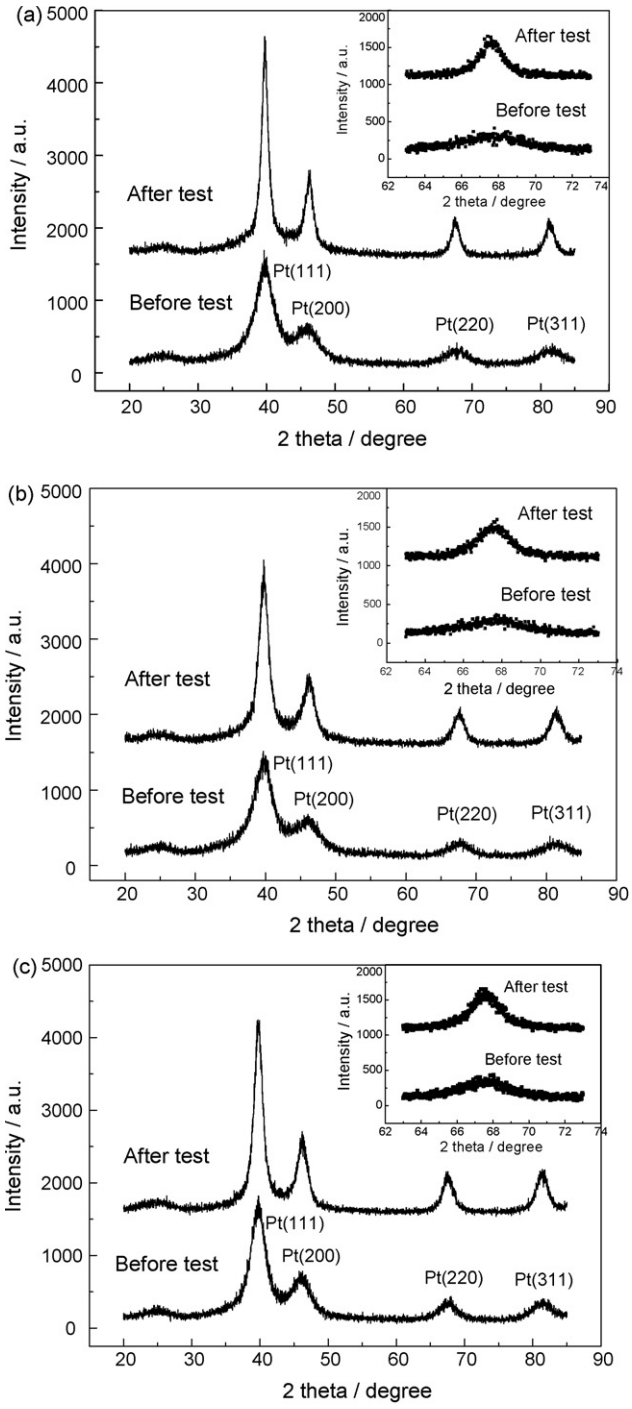

Fig. 4. X-ray diffraction patterns of Pt/C catalysts before and after the potential cycling test. (a) Pt/Vulcan; (b) Pt/Vulcan-O; (c) Pt/Vulcan-N. The insets are Pt(2 2 0) peaks.

The degradation of nano-sized Pt-based catalysts under the electrochemical stress has been widely studied recently

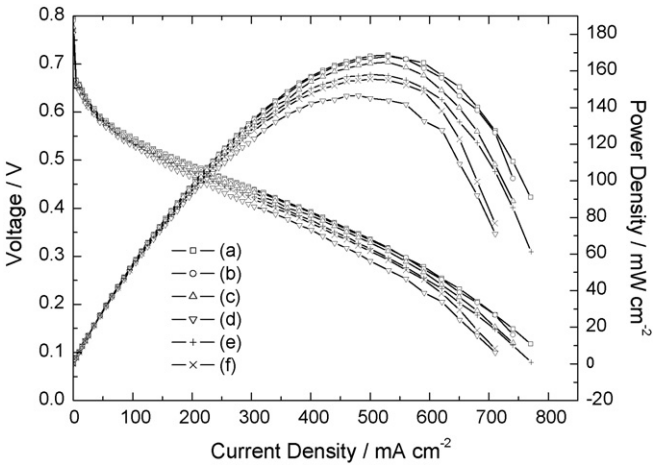

Fig. 5. Polarization curves of the DMFC single cell. 75 °C; anode: 1 mol l^{-1} methanol solution; cathode: 0.2 MPa O_2. Cathode catalysts: (a) Pt/Vulcan before potential cycling; (b) Pt/Vulcan-O before potential cycling; (c) Pt/Vulcan-N before potential cycling; (d) Pt/Vulcan after potential cycling; (e) Pt/Vulcan-O after potential cycling; (f) Pt/Vulcan-N after potential cycling.

[10,19–23]. For supported metal catalysts, the interaction between the metal particle and the support is of great importance to the electrochemical stability. Shao et al. [24,25] investigated the durability of carbon black-supported Pt (Pt/C) and multi-walled carbon nanotubes supported Pt (Pt/CNTs) catalysts using an accelerated durability test, and found that Pt particles in Pt/CNTs present a higher sintering resistance than in Pt/C. The high stability of Pt/CNTs is attributed to the specific interaction between Pt and the support. Prado-Burguete et al. [26] studied the effect of oxygen surface groups of the support on the thermal stability of Pt/C catalysts. The results show that the resistance to sintering is a function of the number of oxygen surface groups of the support. They found that the ease of migration of Pt particles is significantly less for carbon containing oxygen surface groups, and the carbon–platinum interaction is important in restricting the migration of Pt and thus hindering the sintering. Hull et al. [27] investigated the interaction between the Pt nanoparticle and the functionalized multiwalled carbon nanotube with XPS, EXAFS and ATR-IR, and found that the Pt nanoparticles bind to the CNTs via bonding with ester and carbonyl O atoms in the form of COO(Pt) and C(=O)CO(Pt). So it might be concluded that the sintering rate of supported catalysts strongly depends on the interaction between the metal particle and the support.

The polarization curves of the DMFC are shown in Fig. 5. It is seen that after the potential cycling test, the cell performance declined noticeably, and Pt/Vulcan-O and Pt/Vulcan-N displayed higher stabilities than Pt/Vulcan. This result is in accordance with the TEM and XRD results.

4. Conclusions

The agglomeration of the Pt/C catalysts was hindered to some extent by oxidative treatments of the carbon support. A reasonable explanation is that the oxidative treatments make the support surface rich in functional groups, and these functional groups increase the interaction between the metal particle and the support. The HNO_3 treatment normally produces both weak acid groups and strong acid groups on the support surface, while the H_2O_2 treatment primarily produces weak acid groups, which strongly increase the interaction between the metal particle and the support. It is suggested that treating the carbon support with less acidic oxidizers such as H_2O_2 is a useful method for improving the stability of carbon-supported metal catalysts.

Acknowledgements

This work was financially supported by the National High-tech Development Program of China (grant no. 2006AA03Z225) and the Educational Department of Liaoning Province, China.

References

[1] L. Carrette, K.A. Friedrich, U. Stimming, ChemPhysChem 1 (2000) 162–193.
[2] A.S. Aricò, S. Srinivasan, V. Antonucci, Fuel Cells 1 (2001) 133–161.
[3] M.A.J. Cropper, S. Geiger, D.M. Jollie, J. Power Sources 131 (2004) 57–61.
[4] S. Wasmus, A. Küver, J. Electroanal. Chem. 461 (1999) 14–31.
[5] M.S. Wilson, F.H. Garzon, K.E. Sickafus, S. Gottesfeld, J. Electrochem. Soc. 140 (1993) 2872–2877.
[6] J. Xie, D.L. Wood III, K.L. More, P. Atanassov, R.L. Borup, J. Electrochem. Soc. 152 (2005) A1011–A1020.
[7] G. Wu, Y.S. Chen, B.Q. Xu, Electrochem. Commun. 7 (2005) 1237–1243.
[8] R. Yu, L. Chen, Q. Liu, J. Lin, K.L. Tan, S.C. Ng, H.S.O. Chan, G.Q. Xu, T.S.A. Hor, Chem. Mater. 10 (1998) 718–722.
[9] P. Yu, M. Pemberton, P. Plasse, J. Power Sources 144 (2005) 11–20.
[10] H.R. Colón-Mercado, B.N. Popov, J. Power Sources 155 (2006) 253–263.
[11] C.H. Paik, G.S. Saloka, G.W. Graham, Electrochem. Solid-State Lett. 10 (2007) B39–B42.
[12] Z. Zhou, S. Wang, W. Zhou, G. Wang, L. Jiang, W. Li, S. Song, J. Liu, G. Sun, Q. Xin, Chem. Commun. (2003) 394–395.
[13] G.C. Torres, E.L. Jablonski, G.T. Baronetti, A.A. Castro, S.R. de Miguel, O.A. Scelza, M.D. Blanco, M.A. Pena Jimenez, L.J.G. Fierro, Appl. Catal. A 161 (1997) 213–226.
[14] J.L. Gómez de la Fuente, M.V. Martínez-Huerta, S. Rojas, P. Terreros, J.L.G. Fierro, M.A. Peña, Carbon 43 (2005) 3002–3005.
[15] A.E. Aksoylu, M. Madalena, A. Freitas, M. Fernando, R. Pereira, J.L. Figueiredo, Carbon 39 (2001) 175–185.
[16] J.L. Gómez de la Fuente, S. Rojas, M.V. Martínez-Huerta, P. Terreros, M.A. Peña, J.L.G. Fierro, Carbon 44 (2006) 1919–1929.
[17] V. Radmilović, H.A. Gasteiger, P.N. Ross, J. Catal. 154 (1995) 98–106.
[18] A.E. Aksoylu, M. Madalena, A. Freitas, J.L. Figueiredo, Appl. Catal. A 192 (2000) 29–42.
[19] X. Cheng, L. Chen, C. Peng, Z. Chen, Y. Zhang, Q. Fan, J. Electrochem. Soc. 151 (2004) A48–A52.
[20] W. Chen, G. Sun, J. Guo, X. Zhao, S. Yan, J. Tian, S. Tang, Z. Zhou, Q. Xin, Electrochim. Acta 51 (2006) 2391–2399.
[21] A. Taniguchi, T. Akita, K. Yasuda, Y. Miyazaki, J. Power Sources 130 (2004) 42–49.
[22] W. Chen, G. Sun, Z. Liang, Q. Mao, H. Li, G. Wang, Q. Xin, H. Chang, C. Pak, D. Seung, J. Power Sources 160 (2006) 933–939.

[23] R.L. Borup, J.R. Davey, F.H. Garzon, D.L. Wood, M.A. Inbody, J. Power Sources 163 (2006) 76–81.
[24] Y. Shao, G. Yin, Y. Gao, P. Shi, J. Electrochem. Soc. 153 (2006) A1093–A1097.
[25] Y.Y. Shao, G.P. Yin, Y.Z. Gao, Acta Chim. Sinica 64 (2006) 1752–1756.
[26] C. Prado-Burguete, A. Linares-Solano, F. Rodríguez-Reinoso, C. Salinas-Martínez de Lecea, J. Catal. 115 (1989) 98–106.
[27] R.V. Hull, L. Li, Y. Xing, C.C. Chusuei, Chem. Mater. 18 (2006) 1780–1788.